

Predictions for Coefficients of Thermal Expansion of Three-Dimensional Braided Composites

Soheil Mohajerjasbi*

Boeing Defense & Space Group, Philadelphia, Pennsylvania 19142-0858

A finite element- (FE-) based method for prediction of the coefficients of thermal expansion of three-dimensional braided composites is introduced. Since the yarn structure of three-dimensional braided composites is different from that of laminated composites, the fiber architecture of three-dimensional braided composite is briefly reviewed. This FE-based method takes into account the different fiber architectures in the interior, boundaries, and the corners of the braided composite and treats the yarns and the matrix as distinct FEs, with no smearing as is customary in lamination theory. The FE model of the composite is obtained by superposition of these FE models and application of certain constraints. The variation of axial coefficient of thermal expansion of three-dimensional braided composite with interior braiding angle is shown to have a similar form as that of angle-ply laminate. Finally, predictions of this modeling approach for variation of coefficients of thermal expansion of three-dimensional braided composite with different percentages of axial yarns are presented. These theoretical predictions need to be verified by experiments.

Introduction

THE thermoelastic properties of three-dimensional braided composites are of interest and are being investigated because of the cost saving potential offered by this class of composites. The potential of braided composites in reducing cost is envisioned in the ability to manufacture near-net-shape parts, and the ability to use fiber and matrix in their lowest cost form. However, to realize this cost saving potential, the process of preform fabrication needs to be automated and resin impregnation and consolidation processes such as resin transfer molding need to be further developed. Preforms of a wide range of complex geometric shapes may be produced by the three-dimensional braiding process. The composites manufactured by this process exhibit superior delamination resistance and good energy absorbing capability. This process is not without limitations, however; the presently available braiding machines are not fully automated and are relatively slow, and the size of the parts that can be produced with this process is limited by the physical dimensions of the braiding machine.

In the fabrication of composites, one of the causes of residual stresses is large temperature changes between fabrication temperature and room temperature. Also, additional thermal stresses are induced in the composite whenever the temperature of the composite differs from room temperature. Knowledge of thermoelastic properties is important as composite materials are designed to operate in different environments.

A finite element- (FE-) based methodology for calculation of coefficients of thermal expansion of three-dimensional braided composites is presented. Because the fiber architecture of three-dimensional braided composites is different from the conventional laminated composites, the fiber architecture of three-dimensional braided composite is briefly reviewed before introducing this methodology. Somewhat more detailed information on the operation of the braiding machine and resulting fiber architecture of the preform is included as an Appendix. This FE-based method treats the yarns and the matrix as distinct FEs, with no smearing as is customary in lamination theory. The FE model of the composite is obtained by superposition of these FE models and the application of certain constraints. The predictions of this modeling approach for the variation of coefficients of thermal expansion of three-dimensional braided composite with different percentages of axial yarns as a function of interior braiding angle is presented.

Coefficients of Thermal Expansion

The operation of the braiding machine and resulting fiber architecture of three-dimensional braided composite is briefly explained in the Appendix; however, as an introduction to the discussion of the proposed modeling approach, the fiber architecture of the preform is reviewed here. The yarns in the interior of the preform assume two different formations (shown in Fig. 1), which are characterized by interior braiding angle γ measured with respect to the axis of the braided preform (z axis). In the interior of the preform, the two yarn formations alternate along 45 and 135 deg measured from the x axis, and they also alternate along the z axis. Three parameters, u , v , and w , which may be measured from the surfaces of the braided composite, uniquely define the interior braiding angle. Because of the continuity of the yarns in the preform, each yarn from the interior enters the boundary and over a distance h , known as a pitch, changes direction, and enters the interior again. Similarly, each yarn that enters the corner from the interior, changes direction, and over a distance of $3h/2$ enters the interior again. As a result, the fiber architecture at the boundaries and corners are different from the interior.

The yarn structure of the braided composite produced in four machine steps is referred to as a repeat unit because any subsequent machine operation is a repeat of these four steps and will produce a yarn structure that is identical to the one produced in these four steps. Following the convention introduced in Fig. 2, the structure of the interior of the braided composite may be presented as shown in Fig. 3, and the complete repeat unit may be shown in terms of interior cells, boundary cells, and corner cells, as shown in Fig. 4. Note that as the number of yarn carriers increase (with corresponding increase in the size of the preform), a larger percentage of the preform will be composed of the interior cells.

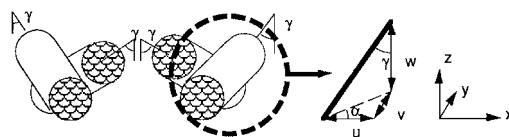


Fig. 1 Yarn arrangement in the interior of three-dimensional braided composite.

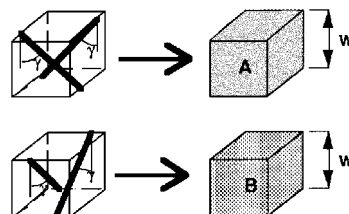


Fig. 2 Interior yarn formations shown as type A and type B cells.

Received Jan. 30, 1996; revision received Sept. 8, 1996; accepted for publication Sept. 14, 1996; also published in *AIAA Journal on Disc*, Volume 2, Number 1. Copyright © 1996 by The Boeing Company. Published by the American Institute of Aeronautics and Astronautics, Inc., with permission.

*Staff Engineer, Helicopters Division. Member AIAA.

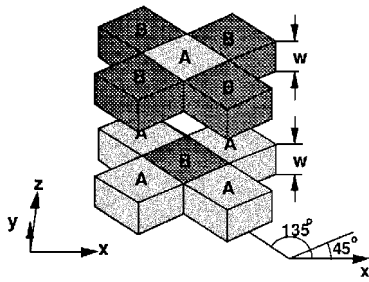


Fig. 3 Interior of the braided composite represented as cells type A and type B.

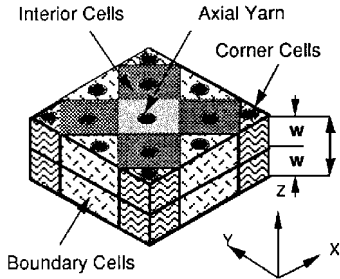


Fig. 4 Repeat unit of three-dimensional braided composite.

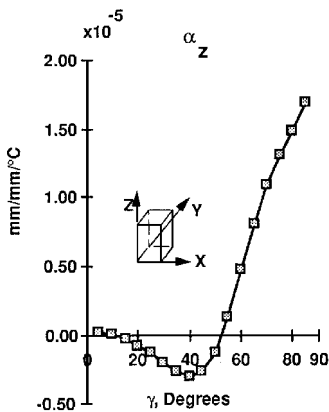


Fig. 5 Coefficient of thermal expansion of three-dimensional braided GR/E with 50% fiber volume fraction.

The properties of the repeat unit (shown in Fig. 4) are considered to represent the properties of the three-dimensional braided composite. MSC/NASTRAN, a commercially available FE code, is used to model the structure of the repeat unit. The geometry of the model is defined by grid points on three planes, which correspond to the lower, middle, and the upper planes of the repeat unit, and represent the corner points of the type A and type B interior cells (Fig. 2) and the boundary and corner cells. The coordinates of these grid points are completely described by the parameters u , v , and w (Figs. 1 and 4). The braiding yarns are modeled using axial elements with axial stiffness only (ROD). The matrix is modeled using solid elements (HEXA and PENTA) with isotropic properties. Constraint equations (MPC) are written to tie the degrees of freedom at the ends of the axial elements to their corresponding points on the solid elements. It is noted that the model representing the braided composite is a superposition of two FE models that are tied together with the constraint equations (MPC). By treating the three-dimensional braided composite in this manner, displacement compatibility between the axial elements and the solid elements only exists at the endpoints of the axial elements and not at any other intermediate point along their length.

The FE model constructed in this manner is constrained to remove the rigid-body motion. Then, the coefficients of thermal expansion are found by applying 1° temperature in the absence of mechanical loads to the model and calculating the resulting strain. The average normal strain in any direction is calculated from the average nodal displacements of the opposite faces of the model in that direction and the dimensions of the model.

The predictions of this model for the coefficient of thermal expansion in the axial direction of a three-dimensional braided composite made of graphite/epoxy (GR/E) with $v_f = 0.50$ is shown in Fig. 5. The shape of this curve suggests that for a range of interior braiding angles from about 15 to 50 deg the axial coefficient of thermal

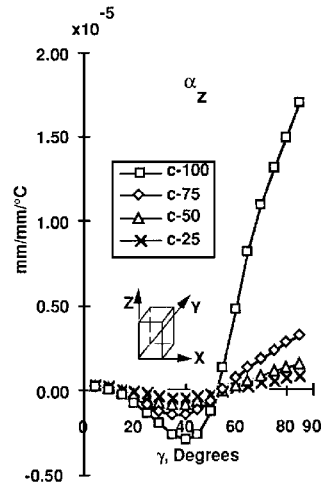


Fig. 6 Axial coefficient of thermal expansion of a three-dimensional braided composite with different percentages of axial yarns.

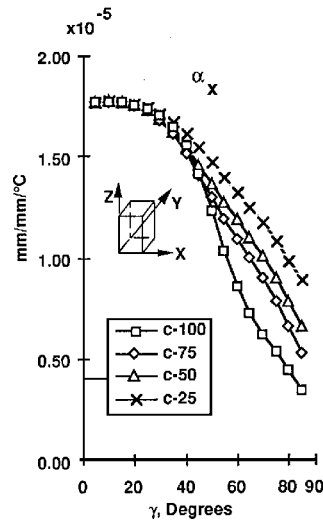


Fig. 7 Transverse coefficient of thermal expansion of three-dimensional braided composite with different percentages of axial yarns.

expansion is negative. Any temperature rise will then produce a contraction of the braided composite in the axial direction. A similar form was obtained for the variation of axial coefficient of thermal expansion of angle-ply laminates,¹ as was previously observed by Halpin and Pagano² in their study of environmentally induced expansional strains.

The same methodology was employed to make predictions for the coefficients of thermal expansion of three-dimensional braided composite with different percentages of axial yarns. The FE model that was explained was modified to include axial yarns (directed along the z direction). As before, axial elements (ROD) were used to model these axial yarns and constraint equations (MPC) were written to tie the degrees of freedom at the endpoints of these axial yarns to their corresponding nodes of the solid elements. The predictions of the model for the variation of axial and transverse coefficients of thermal expansion of a three-dimensional braided composite with different percentages of axial yarns are shown in Figs. 6 and 7, respectively. The predictions of this modeling approach for the elastic constants were reported previously.^{3,4}

In Figs. 6 and 7, c-100 denotes 100% braided with no axial yarns, c-75 denotes 75% braided and 25% axial yarns, c-50 denotes 50% braided and 50% axial yarns, etc. From the variation of coefficients of thermal expansion in the axial and transverse direction shown in Figs. 6 and 7 the following is noted.

1) For a range of interior braiding angles from 15 to 50 deg, the braided composite will contract in the axial direction when heated. This axial shrinkage is accompanied by expansion in the transverse direction.

2) As the interior braiding angle becomes small (close to zero), the braided composite resembles a unidirectional composite. As expected, the model predictions for all axial yarn percentages converge to approximately the same value, which represents the properties of a unidirectional composite with the same fiber volume fraction.

3) With increasing percentages of axial yarns, the curves approach a horizontal line (not shown to avoid clutter), which represents the unidirectional properties. At this limit all properties become independent of the interior braiding angle.

4) The relative change between the curves labeled c-100 and c-75 (in Fig. 6) is more pronounced than between curves labeled c-75 and c-50, etc. This suggests that the introduction of the first 25% axial yarns into the braided preform has a greater effect on the axial coefficient of thermal expansion than subsequent introduction of more axial yarns.

5) The model predictions for the coefficients of thermal expansion are presented for a range of interior braiding angles from 0 to 90 deg. However, in practice, three-dimensional braided preforms can not be braided in the entire range.

Summary and Recommendations

An FE-based method for modeling the behavior of three-dimensional braided composite and calculation of its coefficients of thermal expansion is briefly explained. The predictions of the model for the variation of axial coefficient of thermal expansion of three-dimensional braided GR/E composite with 50% fiber volume fraction is presented. It is noted that these predictions have a form similar to the variation of coefficient of thermal expansion of angle-ply laminate.

Also, the predictions of this modeling approach for the variation of coefficients of thermal expansion of three-dimensional braided GR/E composite with 50% fiber volume fraction and different percentages of axial yarns are presented. It is shown that the trends predicted by this modeling approach appear reasonable; however, these theoretical predictions need to be verified experimentally.

In spite of the availability of analytical models for prediction of the thermoelastic properties, attempts in modeling the strength of this class of composites have not been successful. Future research should be directed to modeling strength and correlating with test data. Once strength models are developed and experimentally verified, design guidelines may be established to help in designing three-dimensional braided parts with the required stiffness and strength.

Appendix: Fiber Architecture of Three-Dimensional Braided Preform

A schematic of a three-dimensional Cartesian braiding machine is shown in Fig. A1. The plane identified as the X - Y plane is referred to as the machine bed and movements of the yarn carriers take place on this plane. The yarn carriers are arranged in rows and columns on the machine bed to form a shape similar to the shape of the preform to be produced. Additional yarn carriers are then added to the outside of this array in alternating locations. The ends of the yarns are tied to a moveable plate above the braiding machine. Movements of the yarn carriers on the machine bed in a prescribed manner will produce the braided preform above the machine at the location shown as the x - y plane. It is possible to add stationary yarns on the braiding machine. These yarns, referred to as axial yarns, will be directed along the length of the preform. For the purpose of demonstration, a process is chosen where the yarn carriers are moved by one carrier spacing in the x and then the y direction in each machine step. This braiding process is referred to as (1×1) and/or four-step process because identical carrier configuration is obtained after each four machine steps.

For sake of illustration of the yarn structure of the braided preform, a square preform with four yarn carriers on each side of the array on the machine bed is considered. The original carrier configuration is shown in Fig. A2. The numbers on the fiber carriers are for the following explanation and otherwise have no significance. For the moment the axial yarns will be ignored as their orientation in the preform is known. Once the fiber architecture of the braided yarns is shown, these axial yarns will be included. The carrier configurations during the four machine steps are demonstrated in Fig. A3.

In the first step the rows identified by leftmost carriers 1 and 2 (Fig. A2) are moved to the right by one carrier spacing, while the rows identified by rightmost carriers 23 and 24 are moved to the left by one carrier spacing. This will result in carrier configuration shown in Fig. A3a. In step 2, columns identified by top carriers 3

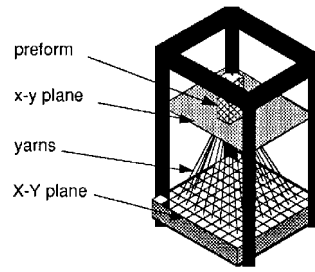


Fig. A1 Schematic of a three-dimensional Cartesian braiding machine.

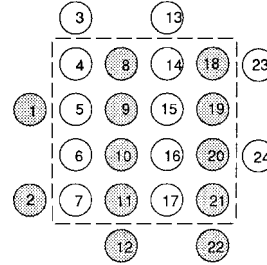


Fig. A2 Original carrier configuration: step 0.

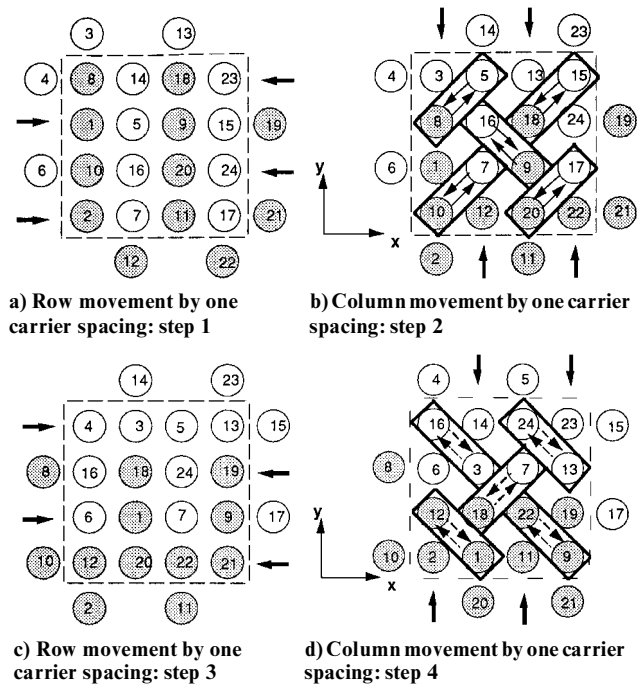


Fig. A3 Machine movements in four-step process.

and 13 (Fig. A3a) are moved down by one carrier spacing, while columns identified with bottom carriers 12 and 22 are moved up by one carrier spacing. In step 3, rows identified by leftmost carriers 4 and 6 are moved to the right by one carrier spacing, while rows identified by rightmost carriers 19 and 21 are moved to the left by one carrier spacing. In step 4, columns identified by the top carriers 14 and 23 are moved down by one carrier spacing, while columns identified by the bottom carriers 2 and 11 are moved up by one carrier spacing. It can be seen that the carrier configurations in Fig. A2 and Fig. A3d are identical; i.e., the carrier configuration repeats itself after four steps, hence the name four-step braiding. Any subsequent machine movement in producing more preform is simply a repeat of the four steps already explained.

A comparison of Figs. A2 and A3b shows that during the first two machine steps the carriers that are shown in boxes switch places. Because the motion of the upper end of the yarns is constrained, as a result of switching places of the carriers shown in the first two steps, the yarns in the interior of the preform produce two different yarn formations (shown in Fig. 1). These two yarn formations are characterized by angle γ , measured with respect to the axis of the braided preform, which is referred to as interior braiding angle. It can be

seen that these two yarn formations are not identical but a certain symmetry exists between them. From Fig. A3b it is also noted that the two yarn formations alternate along 45 and 135 deg measured from the x axis. Also, a comparison of Figs. A3b and A3d shows that during the third and fourth machine steps the carriers that are shown in boxes switch places. As a result, similar yarn formations but in a different order are produced during the third and fourth steps. From a comparison of Figs. A3b and A3d it is noted that the two yarn formations alternate along the axis of the braiding machine (z axis) as well. Based on similar observations of the movements of the carriers on the machine bed, the fiber architecture at the boundaries and corners of the preform are also determined. Because of the continuity of the yarns in the preform, each yarn from the interior enters the boundary and over a distance h , known as a pitch, changes direction, and enters the interior again. Similarly, each yarn that enters the corner from the interior, changes direction, and over a distance of $3h/2$ enters the interior again. As a result, the fiber architecture at the boundaries and corners are different from the interior. The fiber architecture at the boundaries and corners of the preform are shown in Ref. 5.

The interior fiber architecture of the braided composite may be better demonstrated if the two interior yarn formations (Fig. 1), after consolidation with matrix material, are represented as type A and type B cells, as shown in Fig. 2.

In Fig. 2 the dark inclined lines inside the cubes represent the braiding yarns, and the cubes represent the matrix material. The yarns are reduced in size and represented by their centerline, to avoid clutter and provide visibility into the cells. Using these definitions for the two cell types, the interior of the braided composite that is formed in four machine steps may be represented as shown in Fig. 3. The upper part corresponds to the preform formed in the first two machine steps, and the lower part corresponds to the preform

formed in the last two steps. The two cell types alternate along directions 45 and 135 deg measured from the x axis, and they also alternate along the z axis. Any subsequent machine operation is a repeat of these four steps and will produce a yarn structure that is identical to the one produced in these four steps. The axial yarns that were ignored until now for convenience may be represented as vertical lines (directed along the z axis). The structure of the braided composite produced in four machine steps is referred to as a repeat unit. Following the convention of type A and type B cells (Fig. 2) the structure of this repeat unit may be shown in terms of interior cells, boundary cells, and corner cells, as shown in Fig. 4.

References

- ¹Mohajerjasbi, S., "Predictions for Coefficients of Thermal Expansion of 3-D Braided Composites," *Proceedings of the AIAA/ASME/ASCE/AHS/ASC 37th Structures, Structural Dynamics, and Materials Conference* (Salt Lake City, UT), AIAA, Washington, DC, 1996, pp. 1812–1817 (AIAA Paper 96-1531).
- ²Halpin, J. C., and Pagano, N. J., "Consequences of Environmentally Induced Dilatation in Solids," U.S. Air Force Materials Lab., AFML-TR-68-395, Wright-Patterson AFB, OH, 1968.
- ³Mohajerjasbi, S., "Modeling and Analysis of 4-Step Cartesian Braided Composites Including Axial Yarns," *Proceedings of the AIAA/ASME/ASCE/AHS/ASC 36th Structures, Structural Dynamics, and Materials Conference* (New Orleans, LA), AIAA, Washington, DC, 1995, pp. 8–16 (AIAA Paper 95-1157).
- ⁴Mohajerjasbi, S., "Structure and Properties of Three-Dimensional Braided Composites Including Axial Yarns," *AIAA Journal*, Vol. 34, No. 1, 1996, pp. 209–211.
- ⁵Mohajerjasbi, S., "Analytical Models for Prediction of Thermoelastic Properties of 3-D Braided Composites—A Review," *Proceedings of the Symposium on Innovative Processing and Characterization of Composite Materials*, edited by R. F. Gibson, T. W. Chou, and P. K. Raju, American Society of Mechanical Engineers, New York, 1995, pp. 329–342.